STRUCTURE AND MECHANICAL PROPERTIES OF STRESS-ORDERED Ni_4Mo

A THESIS

Presented to

The Faculty of the Graduate Division

by

Keh-Chang Chen

In Partial Fulfillment

of the Requirements for the Degree

Master of Science in Metallurgy

Georgia Institute of Technology

January, 1973

STRUCTURE AND MECHANICAL PROPERTIES OF
STRESS-ORDERED Ni_4Mo

Approved:

Chairman

Date approved by Chairman 3/1/73

ACKNOWLEDGMENT

The author wishes to express his gratitude to his thesis advisor, Dr. E. A. Starke, Jr., for his helpful advice, continuous encouragement and patience during the course of this thesis. He also wishes to thank Drs. B. G. LeFevre and H. Grenga for their careful reading of the manuscript and their thoughtful advice.

The author's grateful appreciation is expressed to Dr. Fu-Wen Ling for his invaluable assistance and useful suggestions. The financial support of this project by the United States Atomic Energy Commission, under contract number AT-(40-1)-3908, is also gratefully acknowledged.

Finally, special thanks are given to the author's fiancee, Mei-luan for her patience and understanding during these trying times.

TABLE OF CONTENTS

LIST OF TABLES

LIST OF FIGURES

SUMMARY

The ordering of Ni_4Mo by isothermal annealing with and without an applied stress at 700°C has been studied. The microstructural features developed during ordering have been correlated with the mechanical properties. Ordering under an applied stress effects both the kinetics and the number of c-axes variants which exist within any one grain. The number of variants has an influence on the mechanical behavior.

CHAPTER I

INTRODUCTION

Ni_4Mo exhibits a face-centered cubic disordered structure (α phase) above the order-disorder transformation temperature, 868°C,[1] and forms a body-centered tetragonal ordered structure (β phase) below this temperature. The ordering reaction is accompanied by a 1.19% contraction in the c-axis of the bct structure[2] and a rotation of arctan (1/3) degree with respect to the fcc structure. The c-axis of the superlattice is always parallel to one of the three original axes of the fcc structure, and for each c-axis there are two different rotational angles possible. Therefore, six different orientations or domains, relative to the disordered lattice, may occur. For a normal ordering condition, all six are equally distributed in the crystal except in the neighborhood of a free surface.[3]

Three kinds of domain boundaries may form during ordering. The first is formed by impingement of two domains with the same orientation (parallel c-axes, and same sign rotation angle); the second is formed by two domains with different rotation angles but with parallel c-axes; and the last one is formed by two domains with orthogonal c-axes. These domain boundaries are called antiphase-domain boundaries (APDB), antiparallel-twin boundaries (APTB), and perpendicular-twin boundaries (PTB), respectively. In general, the APDB has the lowest energy of the three since no appreciable distortion occurs except when a Mo-Mo relationship exists across the boundary. The APTB usually contains small strains due

to the irregular distribution of Mo atoms in the boundary. The PTB has the highest energy of all three since the orthogonality of the c-axes of the domains creating the boundaries causes large distortions in the boundaries.[3]

X-ray line broadening analysis has shown that the microstrains which develop during isothermal ordering at 700°C and 650°C are proportional to the tetragonality of the bct superlattice structure and also dependent on the degree of order and domain size.[4] The microstrains are primarily a result of the strain at the PTB produced by the lattice misfit during ordering. Generation of dislocations at the PTB may be possible during the late stages of ordering.[3] This has been verified indirectly by the internal friction studies of Ling, Collado, and Starke.[5]

Both APDB's and PTB's effect the work hardening coefficient, but the presence of PTB's has a more significant influence on the yield strength since microstrains are present at the coherent PTB's. A quantitative analysis of the effects on mechanical properties by these two kinds of boundaries is possible if the fractions of either one can be controlled. For instance, if all c-axes are parallel there will be no PTB. Hirabayashi[8] investigated the influence of a small stress applied during the ordering anneal on the dimensional change accompanying ordering of CuAu and found that a change in distribution of domain orientation had been affected by the stress. He also verified that an applied compressive stress will favor the development of that domain orientation which most effectively contracts the crystal along the compressive axis. Arunachalan and Cahn[9] ordered CuAu single crystals under a compressive

stress and were able to orient approximately 90% of the c-axes in the direction of the compressive stress. The 1.19% contraction that occurs along the c-axis during ordering of Ni_4Mo suggests that this alloy might be amenable to stress ordering.

The present study was undertaken to quantitatively characterize the microstructural features, i.e. degree of order, domain size and type, produced by ordering Ni_4Mo with and without an applied stress and to correlate these features with the mechanical behavior.

CHAPTER II

EXPERIMENTAL METHODS

Ni_4Mo alloys were prepared by arc melting high purity nickel and molybdenum on a water-cooled copper hearth under an argon atmosphere. Each alloy was melted eight times to insure adequate mixing of the nickel and molybdenum. The ingots were homogenized in an evacuated quartz tube at 1000°C for one week, quenched in iced water, swaged to a diameter of 0.2 centimeter and cut to lengths of 8 centimeters. They were then heat treated in an evacuated quartz tube at 1000½C for 24 hours to remove the stresses caused by the mechanical deformation, quenched in iced water and chemically polished. Chemical polishing was carried out at 90°C in a solution of 225 ml nitric acid, 150 ml sulfuric acid, 100 ml distillated water and 3 grams of NaCl.

The specimens for stress-free ordering and stress ordering were inserted in quartz tubes and heat treated simultaneously in the center of the aging furnace. Each stress ordered specimen was compressed by a stainless steel rod with a free weight of about 11 kilograms, so that the compressive force would be constant during heat treatment. In order to prevent the diffusion between the contacts of the stainless steel (the rod and the base) and the stress-ordered specimen, two extra pieces of Ni_4Mo alloy were placed at both ends of the specimen within the quartz tube. The specimen under stress was placed as close as possible to the stress-free specimen so that the heat-treating conditions, such as time, temperature and environment, would be the same for both during ordering.

The specimens were ordered for various times by isothermal aging at 700°C. The temperature and times were chosen from previous experience with Ni_4Mo polycrystalline,[10] and single crystal samples.[3] All heat treatments were conducted under vacuum (10^{-5} torr) using the vacuum chamber of an MRC model EVD-97 unit.

The degree of order after various heat treatments was determined from Debye-Scherrer patterns by measuring the integrated intensity with a microphotometer and applying the method of LeFevre and Starke.[11] The order parameter was measured on each tensile sample prior to testing. The average domain size was also determined by x-ray diffraction using Scherrer's equation. The $(110)_T^*$ superlattice peak was used for these calculations and was corrected for strain and instrumental broadening by comparison with the nearby $(211)_T$ fundamental peak.

The tensile tests were conducted on an Instron testing machine using a 2.54 cm extensometer and a strain rate of 0.05 per minute. All specimens were pulled to fracture. Microhardness measurements were made on undeformed samples with a Knoop diamond indenter and a 500 gram load. Samples for electron microscopy studies were cut from the tensile samples prior to testing and electropolished using standard techniques.[12] The thin foils were examined in transmission at 100 KV. Two samples, stress and stress-free ordered after 3000 minutes, were mechanically polished and then chemically or electrically polished. The polarized light photomicrographs of those two samples were taken with a Zeiss microscope.

---

*Subscript T refers to the tetragonal indices; cubic indices are undesignated.

CHAPTER III

RESULTS

The structure and mechanical properties of Ni_4Mo were studied after isothermal ordering, with and without an applied stress at 700°C. The degree of long-range order, average domain size and microstructure were correlated with the tensile and hardness measurements which provided an indication of the strength and work hardening of the alloy at various stages of ordering.

The average domain sizes (D) of two sets of samples, stress-free and stress ordered, after various ordering times (t) are shown in Figure 1 by the characteristic linear relation of the ln D versus ln t plot with a slope of 1/2.8. The domain size, long-range order parameter (S), hardness, yield stress, and work-hardening coefficient, for the stress and stress-free ordered samples after various ordering times, are given in the Table. The work-hardening coefficients were measured at 2% strain from the stress-strain curve. All parameters increase faster with aging time for the stress-ordered samples than for the stress-free-ordered samples. However, the stress-free-ordered samples have higher maximum values of yield stress and work hardening coefficient, and "over-aging" is more pronounced for the times used in this study.

The normals of all the foils examined in the electron microscope were approximately parallel to the stress axis of the stress-ordered samples. All types of domain boundaries were found in both stress-ordered and stress-free-ordered samples. However, perpendicular twins

Table 1. Structural Parameters of SO and SFO Ni_4Mo.

Aging Time (minutes)	LRO Parameter		Domain Size (Å)		Hardness (Knoop)		Yield Stress (kg/cm^2)		Work Hardening Coefficient x 10^3 (kg/cm^2/% strain)	
	SFO*	SO**	SFO	SO	SFO	SO	SFO	SO	SFO	SO
0	0	0	-	-	228	228	3500	3500	1.10	1.10
100	0.75	.82	114	140	394	422	4680	5160	1.29	1.42
400	0.95	1.00	161	221	455	442	6500	6350	1.64	1.60
1000	1.00	1.00	215	270	486	443	7500	6320	1.89	1.62
2000	-	-	-	-	475	436	7050	6330	-	-
3000	1.00	1.00	266	355	455	438	6900	6200	1.61	1.49

* SFO = Stress-free ordered

** SO = Stress Ordered

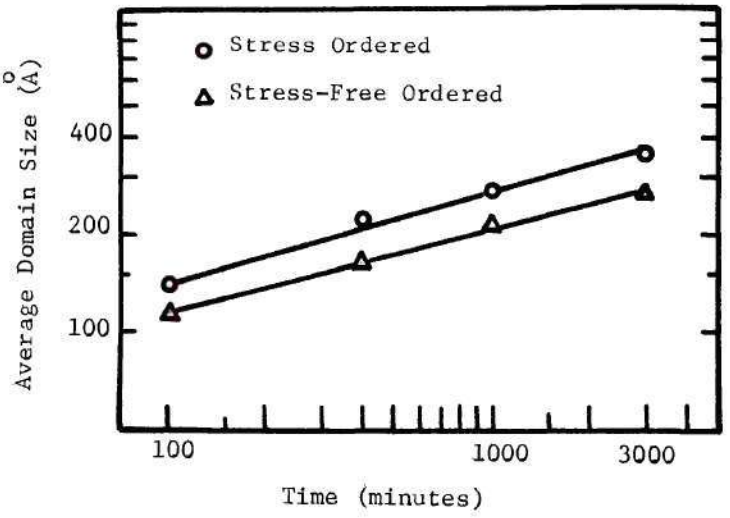

Figure 1. Variation of the Average Domain Size of Ni_4Mo with Aging Time at 700°C.

were much more frequently observed in stress-free-ordered samples than in stress-ordered samples. The following micrographs are designed to explain the different domain structures present in the late ordering stage in Ni_4Mo. The identification of the boundaries is based on the argument of previous workers.[13,14]

Because of the contraction and expansion along the axes, the possible coherent planes for anti-parallel twins are (100), (010), (110) and $(1\bar{1}0)$ since the d spacing remains the same on both sides of the twin boundary. Similarly, the preferred planes for perpendicular twin boundaries are (101) and $(10\bar{1})$.[13] In the early stage of ordering, when S is small, and there has been little or no change in lattice constants, APT and PT boundaries are not necessarily on preferred planes and may appear curved. As the LRO increases the lattice misfit across twin boundaries increases and PT boundaries become more planar as the lower lattice misfit planes become preferred as boundaries. Anti-parallel twin boundaries, which have lower energy than PT boundaries, may remain curved or may become planar depending on the domain's configuration and distribution. The curved APT boundaries can be seen in Figures 2. Planar APT boundaries are observed in Figure 3(a) which is a micrograph of a sample stress-ordered for 1000 minutes at 700°C. The diffraction pattern from the area shown in 3(a), Figure 3(b), shows that two variants with the same c-axes are twin related. Trace analysis suggests that trace A may be parallel to (110), (110)* or (100) planes, and trace B may be parallel to (001), (011), $(00\bar{1})$ planes. This suggestion is based on the assumption that these planes are preferred as APT boundaries.[13]

*The trace analysis is based on the cubic structure and it is not possible to distinguish between (101) and (110) planes.

Figure 2. Dark Field Image With a Superlattice Reflection Showing APB's in Ni_4Mo after 400 Minutes Stress-Free Ordering at 700°C (50,000X).

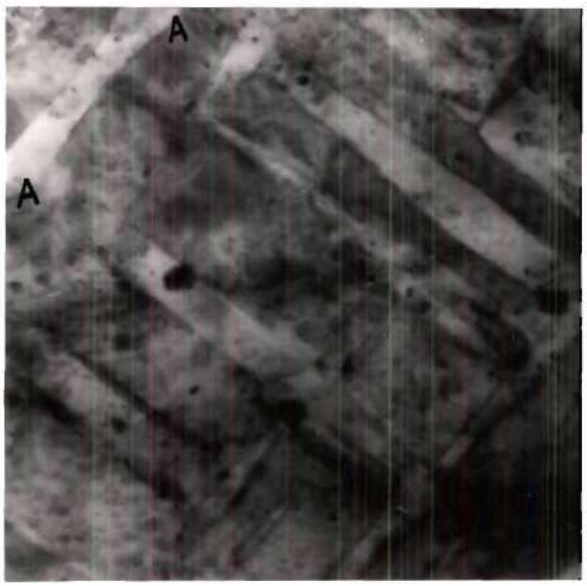

(a) Bright Field Electron Micrograph, [150] Orientation; Antiphase Parallel Twin Structures (22,000X).

Figure 3. Ni_4Mo Stress Ordered for 1000 Minutes at 700°C.

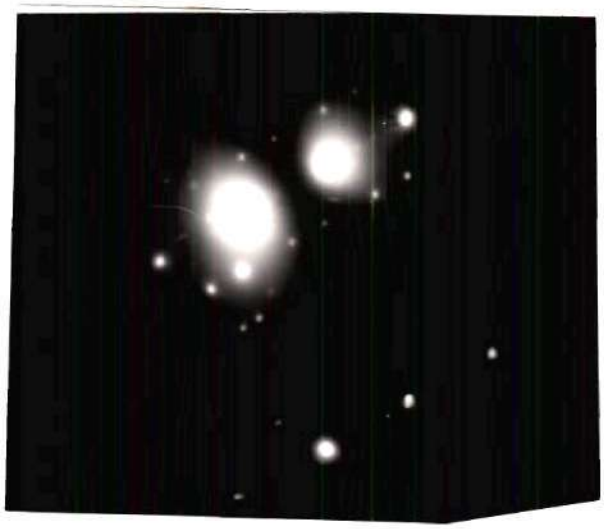

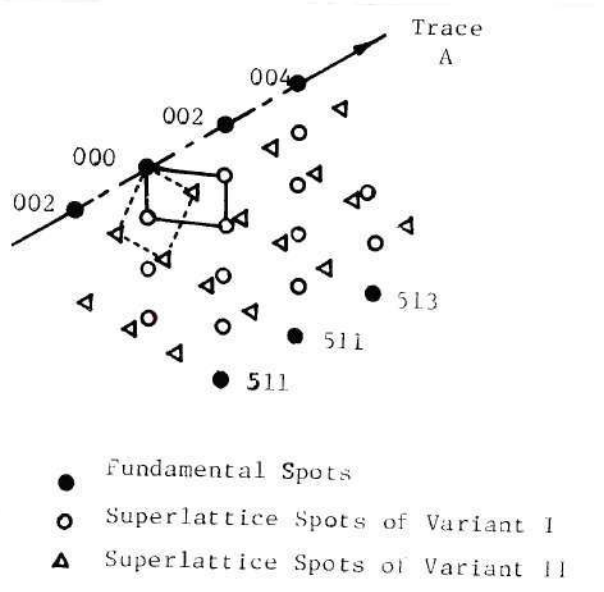

Figure 3(b) Diffraction Pattern from Area Shown in (a) (Cubic Indices are Used).

Figure 4(a) shows perpendicular twin boundaries present in the stress-free-ordered sample after 1000 minutes at 700°C. A comparison of the diffraction pattern from the area shown in 4(a), Figure 4(b), with a reciprocal lattice model containing all variants, showed that the pattern results from two variants of mutually perpendicular c-axes. A trace analysis suggests that the boundaries may be parallel to {101} planes as previously suggested.

The perpendicular twin boundary may become partially incoherent after long ordering times because of the misfit strain in the perpendicular twin plane. Therefore, after the twin boundaries are eliminated by domain growth, the dislocations generated from perpendicular twin boundaries are left within the new domains and form subgrain boundaries as shown in Figure 5. This argument is supported by the fact that these subgrain boundaries are normal to <101> poles, and {101} planes are the preferred planes for perpendicular twin boundaries.

The electro-polished samples revealed details in the polarized light micrographs of the domain structure while the chemically polished sample revealed the incoherent boundaries, such as grain boundaries and incoherent domain boundaries. Photomicrographs of electro-polished stress-ordered and stress-free-ordered samples are shown in Figures 6(a) and 6(b) respectively. Since stress ordering eliminates one or two orientation variants there are fewer domain variants in Figure 6(b) than in Figure 6(a).

Figure 7 shows a chemically polished sample after stress ordering. It is noticed that most grains are dominated by only two domain variants. The plate-like domains are probably perpendicular twins since the perpen-

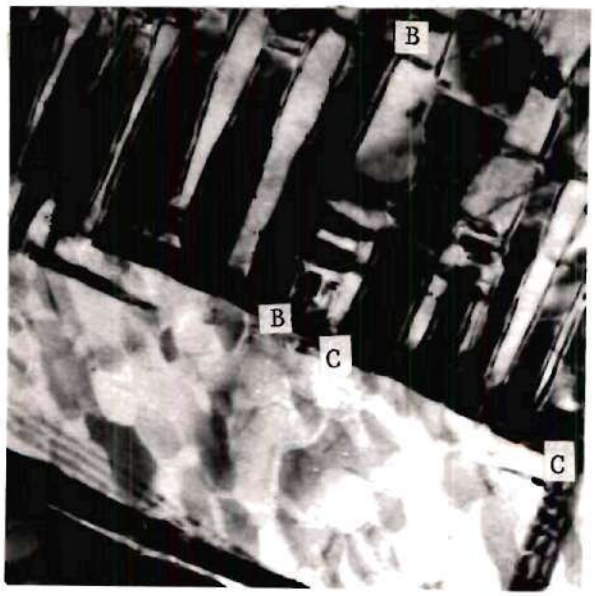

(a) Bright Field Electron Micrograph, $[\bar{1}12]$ Orientation; Perpendicular Twin Structure (40,000X).

Figure 4. Ni_4Mo Stress-Free Ordered for 1000 Minutes at 700°C.

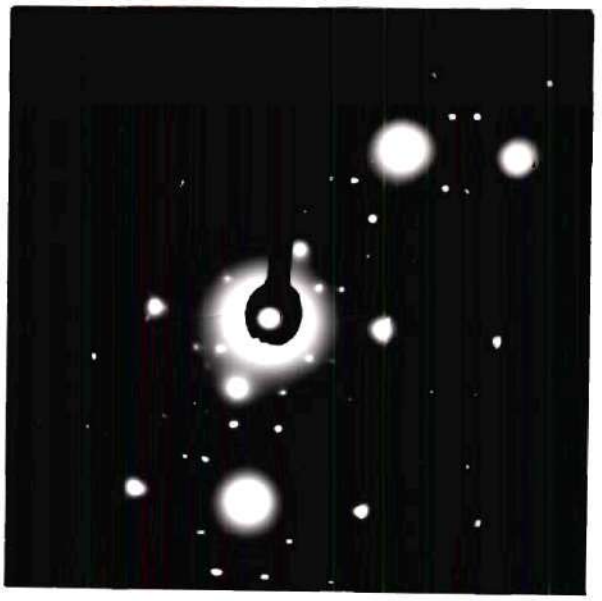

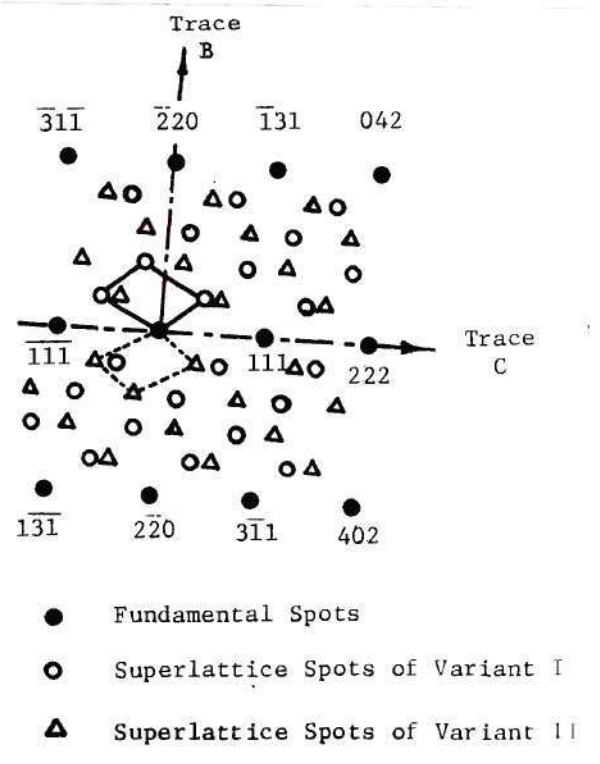

Figure 4(b) Diffraction Pattern from Area Shown in (a) (Cubic Indices are Used).

Figure 5. Bright Field Electron Micrograph of Ni_4Mo Stress-Free Ordered for 1000 Minutes at 700°C [011] Orientation Showing Low Angle Boundaries (40,000X).

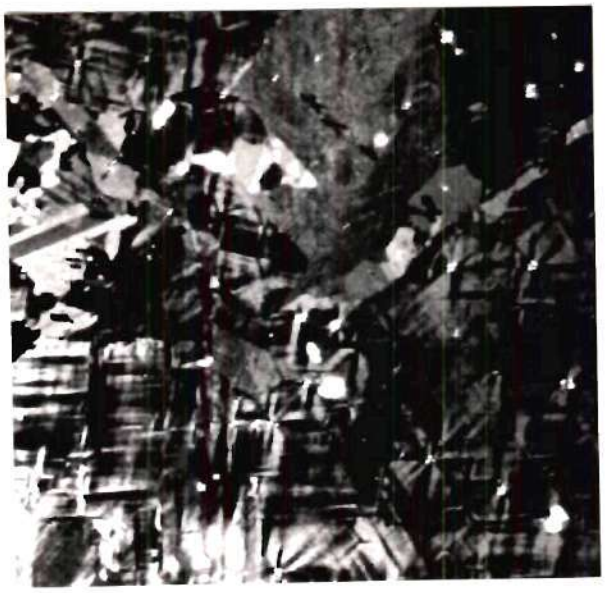

(a)

(b)

Figure 6. The Polarized Light Micrograph of Ni_4Mo After 3000 Minutes of Ordering at 700°C. Samples were Electropolished (320X).

(a) Stress-Free Ordered

(b) Stress Ordered

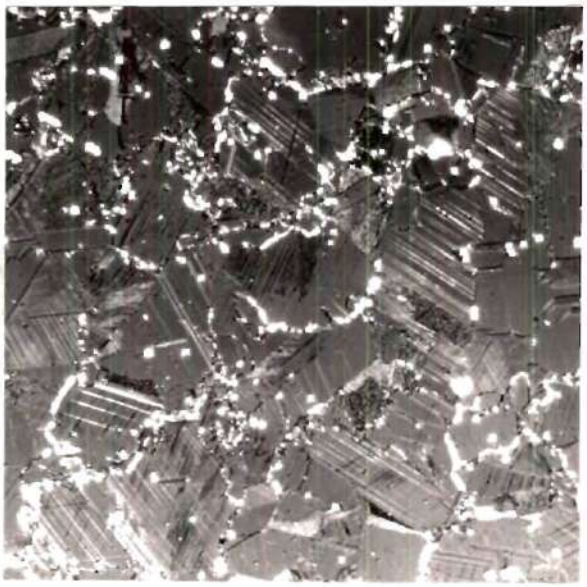

Figure 7. Polarized Light Micrograph of Ni_4Mo After Stress Ordering 3000 Minutes at 700°C. Sample was Chemically Polished (320X).

dicular twin boundaries may become partially incoherent at the very late stage of ordering as described previously. The incoherency of the domain boundaries can be revealed by chemical etching.

CHAPTER IV

DISCUSSION OF RESULTS

The results of this study clearly show that ordering under an applied stress can influence the kinetics of the transformation, the microstructure and mechanical properties of Ni_4Mo. The magnitude of the influence is very orientation dependent, being paramount when the stress axis is parallel to a cube axis but is somewhat averaged in a polycrystalline sample. Theoretically, the application of a uniaxial stress normal to a {111} oriented crystal will not alter the random morphology of the domains since the resolved stresses in the cube directions will be equal in magnitude. Pinhole x-ray patterns of samples used in this study showed them to be randomly oriented with no defined fiber texture.

Two kinds of stress-ordering effects may occur for all of the grains with favorable orientations. The first would occur if any one of the three original cube axes is close to the compression direction. In this case the c-axes of all ordered domains would be oriented in the same direction, i.e. one c-axis variant. The second would occur if one of the <110> poles is close to the compression direction. In this case thw two closer <100> directions for each specific <110> (e.g., [100] and [010] for [110]) would be equally favored, resulting in two c-axes variants. Further orientational relationship may be obtained if the lattice twins in order to relieve ordering stresses.[15,16] Consequently, the probability of obtaining a grain containing domains with only one

c-axis variant (see Figure 6) is small, even for stress-ordered samples. In the stress-free-ordered samples, three c-axes variants normally were observed to coexist within a grain and occasionally two variants, related as perpendicular twins, were observed. Two, twin related, variants were normally observed within grains of the stress-ordered samples; however, occasionally one or three variants were observed. These features were observed by both electron and polarized light microscopy.

The kinetics of the ordering transformation was also seen to be effected by the applied stress. The applied stress tends to lower the transformation strain energy by reducing the probability of PT formation, which increases the change in free energy between the ordered and disordered state resulting in a faster ordering rate, as illustrated in the Table. Domain growth in Ni_4Mo during isothermal ordering has been described by Ling and Starke[3] by the size-time relationship $D^n - D_o^n = K_i t$ where D_o is the initial domain size, D is the domain size at time t, and n and K_1 are constants. The magnitude of n has been suggested to be dependent on alloy purity, decreasing as the purity increases. A value of n = 2.9 was found previously for Ni_4Mo, and the value in the present study is very close to that, being 2.8. The average domain size for the stress ordered samples is larger than that found for the stress-free-ordered samples for the same ordering time. This is probably due to the higher density of PT boundaries inhibiting domain boundary migration for the stress-free ordered samples.

The stress-ordered samples contained fewer PT boundaries than did the stress-free-ordered samples and, consequently, the microstrains caused by lattice misfit are lower in these samples. Therefore the

yield stress and work hardening coefficients are also lower since these parameters are directly related to the microstrains.[3] The higher properties are simply related to the higher degree of order for the stress-ordered samples.

Ling and Starke[3] suggested that the stresses produced by the lattice misfit, in conjunction with thermal fluctuations, can generate dislocations at PT interfaces. This appears to be verified by the electron micrograph shown in Figure 5. The extremely high yield stress of the stress-free-ordered sample after 1000 minutes of ordering can be attributed to internal strains caused by these dislocations.

CHAPTER V

CONCLUSIONS

1. Ordering under an applied stress increases the kinetics of the process due to a reduction in the ordering stresses.

2. The stress-free-ordered samples had higher maximum values of hardness, yield strength and work-hardening rate. This is attributed to three variants existing in most grains of the stress-ordered samples and only two in grains of the stress-free-ordered samples.

3. Dislocations generated from perpendicular twin boundaries can be observed.

BIBLIOGRAPHY

1. P. W. Guthrie, and E. E. Stansbury, Oak Ridge National Laboratory Report ORNL-3078, Oak Ridge, Tennessee, July, 1961.

2. W. B. Pearson, "A Handbook of Lattice Spacing and Structures of Metals and Alloys," Vol. 2, Pergamon Press, New York, 1967.

3. Fu-Wen Ling and E. A. Starke, Jr., Acta Met. 19, 1971, p. 759.

4. Fu-Wen Ling and E. A. Starke, Jr., Advances in X-ray Analysis 15, 1971, p. 319.

5. Fu-Wen Ling, J. Collado and E. A. Starke, Jr., Scripta Met. 6, 1972, p. 307.

6. P. A. Flinn, Trans. AIME 218, 1960, p. 145.

7. G. Schoeck, Acta Met. 17, 1969, p. 147.

8. M. Hirabayashi, J. Phys. Soc. Japan 14, 1959, p. 149.

9. V. S. Arunachalan and R. W. Cahn, "Ordered Alloys," Proceedings of the 3rd Bolton Landing Conference, September, 1969, edited by B. H. Kear et al. Alaitor's Publishing Division, 1970.

10. B. Chakravarti, E. A. Starke, Jr. and B. G. LeFevre, J. of Mater. Sci. 5, 1970, p. 394.

11. B. G. LeFevre and E. A. Starke, Jr., Advances in X-ray Analysis 12, 1969, p. 113.

12. W. B. Snyder, M. S. Thesis, University of Tennessee, August, 1969.

13. E. Ruedl, P. Delavignette and S. Amelinckx, Phys. Status Solidi 28, 1968, p. 305.

14. S. Amelinckx, Surface Science 31, 1972, p. 296.

15. L. E. Tanner, Phys. Stat. Sol. 30, 1968, p. 685.

16. L. E. Tanner, Phys. Stat. Sol. 33, 1969, p. 59.